Pacemaker activity of the rabbit sinoatrial node
A comparison of mathematical models

R. Wilders, H. J. Jongsma, and A. C. G. van Ginneken
Department of Physiology, University of Amsterdam, 1105 AZ Amsterdam, The Netherlands

ABSTRACT In the past decade, three mathematical models describing the pacemaker activity of the rabbit sinoatrial node have been developed: the Bristow-Clark model, the Irisawa-Noma model, and the Noble–Noble model. In a comparative study it is demonstrated that these models, as well as subsequent modifications, all have several drawbacks. A more accurate model, describing the pacemaker activity of a single pacemaker cell isolated from the rabbit sinoatrial node, was constructed. Model equations, including equations for the T-type calcium current, are based on experimental data from voltage clamp experiments on single cells that were published during the last few years. In contrast to the other models, only a small amount of background current contributes to the overall electrical charge flow. The action potential parameters of the model cell, its responses to voltage clamp steps and its current-voltage relationships have been computed. The model is used to discuss the relative contribution of membrane current components to the slow diastolic depolarization phase of the action potential.

INTRODUCTION

The primary pacemaker of the mammalian heart consists of several hundreds or thousands of resistively coupled cells located in the sinoatrial (SA) node (Bleeker et al., 1980; op 't Hof et al., 1985). A large body of information on the ion current systems underlying pacemaker activity has been obtained from voltage clamp experiments on small rabbit SA node preparations containing ~100 cells. This information resulted in three mathematical models of rabbit SA node pacemaker activity: the Bristow-Clark model (Bristow and Clark, 1982), the Irisawa-Noma model (Irisawa and Noma, 1982) and the Noble–Noble model (Noble and Noble, 1984). Recently, Noble et al. (1989) published a modification of the Noble–Noble model, which we shall refer to as the Noble-DiFrancesco-Denyer model. They incorporated new equations for some of the membrane ionic currents based on recent single cell experimental data (DiFrancesco and Noble, 1989).

The denervated SA node shows spontaneous electrical activity with a very regular discharge pattern (Bonke, 1969). Like the intact SA node, individual pacemaker cells isolated from it show spontaneous electrical activity. Their discharge pattern, however, is irregular (op 't Hof et al., 1987). Our hypothesis is that both the irregularity of individual pacemaker cells and the regularity of the intact SA node can be explained in terms of the stochastic open-close kinetics of the membrane ionic channels. To test the validity of this hypothesis we wanted to incorporate the stochastic open-close kinetics of the membrane ionic channels into a mathematical model of electrical activity of a single pacemaker cell.

A satisfactory single cell model, however, was not available. The conversion of the Bristow-Clark model and the Irisawa-Noma model, both multicellular models, into a single cell model is a straightforward operation because all relevant quantities are expressed relative to the membrane area. Each of these models, however, has serious disadvantages which we will discuss below. The multicellular Noble–Noble model can be converted into a single cell model by simply scaling down all, absolute, quantities by a factor of 100, the approximate number of cells comprised in the mulitcellular preparation (Noble et al., 1989). This, however, yields a model which, as we will also discuss below, does not resemble the nowadays available single cell experimental data in several ways. The single cell model resulting from the modification of the Noble–Noble model by Noble, DiFrancesco and Denyer has a number of drawbacks which will also be discussed below. Therefore we developed a single cell model ourselves.

In this paper, at first we give a review of the three above mentioned mathematical models and the single cell modification of the Noble–Noble model. Next we present our model of electrical activity of a single pacemaker cell. The incorporation of the stochastic open-close kinetics into this model will be dealt with in a subsequent paper (in preparation).

0006-3495/91/11/1202/15 $2.00

GLOSSARY

Symbols and units

a_{rel} constant in equation for i_{rel} (in picoamperes/millimolar)

a_{tr} constant in equation for i_{tr} (in picoamperes/millimolar)

a_{up} constant in equation for i_{up} (in picoamperes/millimolar^2)

$\alpha_x, \alpha_y, \ldots$ rate constant of gating variable x, y, ... (in millisecond^{-1})

$\beta_x, \beta_y, \ldots$ rate constant of gating variable x, y, ... (in millisecond^{-1})

C membrane capacitance (in picofarads)

$[Ca^{2+}]_e$ extracellular calcium concentration (in millimolar)

$[Ca^{2+}]_i$ intracellular calcium concentration (in millimolar)

$[Ca^{2+}]_{rel}$ calcium concentration in release store (in millimolar)

$[Ca^{2+}]_{up}$ calcium concentration in uptake store (in millmolar)

$[Ca^{2+}]_{up,max}$ maximum value of calcium concentration in uptake store (in millimolar)

d_L activation gating variable of $i_{Ca,L}$

d_{NaCa} constant in equation for i_{NaCa}

d_T activation gating variable of $i_{Ca,T}$

F Faraday constant (in coulombs/millimol)

f_L inactivation gating variable of $i_{Ca,L}$

f_T inactivation gating variable of $i_{Ca,T}$

$g_{b,Ca}, g_{b,K}, \ldots$ (maximum) conductance for $i_{b,Ca}$, $i_{b,K}$, ... (in nanosiemens)

γ_{NaCa} position of energy peak in equation for i_{NaCa}

h inactivation gating variable of i_{Na}

i_b total background current, comprising $i_{b,Ca}$, $i_{b,K}$ $i_{b,Na}$, and i_{NaK} (in picoamperes)

$i_{b,Ca}$ background calcium current (in picoamperes)

$i_{b,K}$ background potassium current (in picoamperes)

$i_{b,Na}$ background sodium current (in picoamperes)

$i_{Ca,L}$ L-type calcium current (in picoamperes)

$\bar{i}_{Ca,L}, \ldots$ fully-activated $i_{Ca,L}, \ldots$ (in picoamperes)

$i_{Ca,L,Ca}$ calcium component of L-type calcium current (in picoamperes)

$i_{Ca,L,K}$ potassium component of L-type calcium current (in picoamperes)

$i_{Ca,L,Na}$ sodium component of L-type calcium current (in picoamperes)

$i_{Ca,net}$ net calcium current (in picoamperes)

$i_{Ca,T}$ T-type calcium current (in picoamperes)

i_f hyperpolarizing-activated current (in picoamperes)

$i_{f,K}$ potassium component of hyperpolarizing-activated current (in picoamperes)

$i_{f,Na}$ sodium component of hyperpolarizing-activated current (in picoamperes)

i_K delayed potassium current (in picoamperes)

$i_{K,net}$ net potassium current (in picoamperes)

i_{Na} fast sodium current (in picoamperes)

$i_{Na,net}$ net sodium current (in picoamperes)

i_{NaCa} sodium-calcium exchange current (in picoamperes)

i_{NaK} sodium-potassium pump current (in picoamperes)

$i_{NaK,max}$ maximum value of i_{NaK} (in picoamperes)

i_{rel} calcium release current (in picoamperes)

i_{si} slow or second inward current, comprising $i_{Ca,L}$, $i_{Ca,T}$, and i_{NaCa} (in picoamperes)

i_{tot} total current crossing the membrane (in picoamperes)

i_{tr} calcium transfer current (in picoamperes)

i_{up} calcium uptake current (in picoamperes)

$[K^+]_e$ extracellular potassium concentration (in millimolar)

$[K^+]_i$ intracellular potassium concentration (in millimolar)

k_K scaling factor in equation for i_K

$K_{m,b,K}$ constant for potassium activation of $i_{b,K}$ (in millimolar)

$K_{m,Ca}$ constant for activation of calcium release (in millimolar)

$K_{m,Na}$ constant for sodium activation of i_{NaK} (in millimolar)

k_{NaCa} scaling factor in equation for i_{NaCa}

m activation gating variable of i_{Na}

$[Na^+]_e$ extracellular sodium concentration (in millimolar)

$[Na^+]_i$ intracellular sodium concentration (in millimolar)

p "gating variable" representing the time- and voltage-dependence of i_{tr}

$P_{Ca,L}$ calcium permeability of L-type calcium channel, multiplied by F (in picoamperes/millimolar)

$P_{Ca,L,K}$ relative potassium permeability of L-type calcium channel

$P_{Ca,L,Na}$ relative sodium permeability of L-type calcium channel

$P_{Ca,T}$ calcium permeability of T-type calcium channel, multiplied by F (in picoamperes/millimolar)

$P_{Na,K}$ relative potassium permeability of i_{Na} channel

R universal gas constant (in joules mol^{-1} kelvin^{-1})

T temperature (kelvin)

τ_{rel} release time constant for calcium sequestration (in milliseconds)

τ_{tr} transfer time constant for calcium sequestration (in milliseconds)

τ_{up} uptake time constant for calcium sequestration (in milliseconds)

$\tau_x, \tau_y, \ldots$ time constant of gating variable x, y, ... (in milliseconds)

V membrane potential (in millivolts)

V_{Ca} calcium equilibrium potential (in millivolts)

V_i intracellular space volume (in microns^3)

V_K potassium equilibrium potential (in millivolts)

V_{Na} sodium equilibrium potential (in millivolts)

$V_{Na,K}$	reversal potential of i_{Na} (in millivolts)
V_{rel}	volume of calcium release store (in microns^3)
V_{up}	volume of calcium uptake store (in microns^3)
x	activation gating variable of i_K
$x_\infty, y_\infty, \ldots$	steady-state value of gating variable $x, y, \ldots$
y	activation gating variable of i_f

Constants

$C = 32$ pF	$[K^+]_e = 5.4$ mM	$P_{Na,K} = 0.12$
$[Ca^{2+}]_e = 2$ mM	$K_{m,b,K} = 10$ mM	$R = 8.3143$ J mol^{-1} K^{-1}
$[Ca^{2+}]_{up,max} = 5$ mM	$K_{m,Ca} = 0.002$ mM	$T = 310.15$ K
$d_{NaCa} = 0.0001$	$K_{m,Na} = 40$ mM	$\tau_{rel} = 10$ ms
$F = 96.4867$ C/mmol	$[Na^+]_e = 140$ mM	$\tau_{tr} = 200$ ms
$g_{b,Ca} = 0.04$ nS	$i_{NaK,max} = 182$ pA	$\tau_{up} = 5$ ms
$g_{b,K} = 7.5$ nS	$k_K = 11$	$V_i = 5026.5$ μm^3
$g_{b,Na} = 0.15$ nS	$k_{NaCa} = 0.01$	$V_{rel} = 0.02\, V_i$
$g_{f,K} = 7.4$ nS	$P_{Ca,L} = 90$ pA/mM	$V_{up} = 0.05\, V_i$
$g_{f,Na} = 4.6$ nS	$P_{Ca,L,K} = 0.01$	$a_{rel} = 2V_{rel}F/\tau_{rel}$
$g_{Na} = 12.5$ nS	$P_{Ca,L,Na} = 0.01$	$a_{tr} = 2V_{rel}F/\tau_{tr}$
$\gamma_{NaCa} = 0.5$	$P_{Ca,T} = 85$ pA/mM	$a_{up} = 2V_iF/(\tau_{up}[Ca^{2+}]_{up,max})$

METHODS

Action potential parameters

Experimentally recorded action potentials usually are characterized by their cycle length (CL), maximum diastolic potential (MDP), action potential amplitude (APA), action potential duration at 50 and 100% repolarization (APD_{50} and APD_{100}), maximum upstoke velocity ($\dot{V}_{max}$), and diastolic depolarization rate (DDR). Therefore, we will use these seven parameters to characterize the model action potentials too.

Model equations

All models, including the one presented in this paper, are Hodgkin-Huxley type models in that the cell membrane is modeled as a capacitance connected in parallel to a number of conductances representing the ionic channels, their kinetics being described by gating variables representing first-order reaction schemes (Hodgkin and Huxley, 1952). Thus, if not listed explicitly, the equations for the rate constants α_x and β_x of some gating variable x can be inferred from the equations for the time constant τ_x and the steady-state value x_∞ according to

$$\alpha_x = x_\infty/\tau_x,$$

and

$$\beta_x = (1 - x_\infty)/\tau_x.$$

We will use the symbols and units listed in the glossary. The number of ionic channels is assumed to be linearly related to the cell membrane area. Consequently, the maximum current is linearly related to this area too. So one should use current per unit membrane area instead of absolute current to allow for easy comparison. The membrane area, however, can not be measured accurately. Therefore, we have chosen to use the cell membrane capacitance C as a reference: C can be measured accurately and is approximately proportional to the membrane area (Nakayama et al., 1984). Thus, if necessary for comparison, current is expressed in picoamperes/picofarad.

All equations of our model, as well as stable-start values, are given in the appendix. Note that in some of the rate constant equations l'Hospitals rule has to be used. No bounds are put on concentrations. The constants are listed in the glossary.

The equations of the Bristow-Clark model and the Irisawa-Noma model were taken from the papers cited before. Some equations of the Noble–Noble model and the Noble-DiFrancesco-Denyer model could only be obtained by a thorough examination of version 2.1 and version 2.2 of the Oxsoft Heart software package (Oxsoft Ltd., Oxford, England). This package was also used to check the correctness of the remaining equations of these models.

Numerical integration

To calculate the variation of the membrane potential V one has to solve a number of simultaneous first-order differential equations: one for the membrane potential, five for ion concentrations, if not fixed, and, depending on the number of gating variables, six or more equations of the form

$$dx/dt = \alpha_x(1 - x) - \beta_x x.$$

We have applied the accurate and efficient integration method of Victorri et al. (1985). The number of differential equations is considerably reduced by taking

$$x(t + \Delta t) = x_\infty(t) + [x(t) - x_\infty(t)] \cdot \exp[-\Delta t/\tau_x(t)]$$

as an approximate solution to the gating variable equation. At any time t the integration time step Δt is set equal to one of the values $2^n \cdot 0.032$ ms, $0 \le n \le 5$, depending on the computed change in the membrane potential ΔV. If $|\Delta V|$ is greater than 0.4 mV the integration step is repeated with Δt halved until $|\Delta V|$ becomes < 0.4 mV. If $|\Delta V|$ is < 0.2 mV the next integration step is carried out with Δt doubled. The initial value of Δt is 0.032 ms.

EXISTING MODELS

The existing mathematical models differ in the number and kind of membrane current components. Each of the models will now be reviewed in turn. Table 1 gives the model values of the action potential parameters, together with experimentally observed values. Table 2 gives both the absolute and the relative contribution of the membrane current components to the charge flow during spontaneous electrical activity. The dynamics of these current components during spontaneous electrical activity are shown in Fig. 1.

Bristow-Clark model

The Bristow-Clark model (Bristow and Clark, 1982) is a modification of the McAllister-Noble-Tsien model (McAllister et al., 1975). The membrane current components of this cardiac Purkinje fiber model were modified to produce a model that exhibited behavior in agreement with the experimental data published at that time, especially to a "reference transmembrane potential waveform."

Two membrane current components of the Bristow-Clark model are the voltage-dependent, time-indepen-

TABLE 1 **Action potential parameters of a single rabbit SA node cell. Experimentally observed values and model values**

	MDP	APA	CL	APD_{50}	APD_{100}	$\dot{V}_{max}$	DDR
Experimentally observed values	*mV*	*mV*	*ms*	*ms*	*ms*	*V/s*	*mV/s*
Nakayama et al., 1984 (mean ± SD, n = 18)	−53.3 ± 8.2	88.6 ± 10.3	—	100.1 ± 39.4	—	8.5 ± 5.8	—
Hagiwara et al., 1988 (mean ± SD, n = 5)	—	—	296.4 ± 47.5	—	—	—	—
Oei et al., 1989 (mean ± SD, n = 13)	−56 ± 8	—	322 ± 49	91 ± 15	172 ± 30	27 ± 35	79 ± 21
Denyer and Brown, 1990*a* (mean ± SD, n = 12)	−66.2 ± 4.5	97.5 ± 5.5	358.2 ± 136.8	85.8 ± 18.0	—	7.9 ± 2.7	—
van Ginneken and Giles, 1991 (mean ± SD, n = 20)	−57.9 ± 8.0	89.8 ± 9.4	335.4 ± 67.1	72.7 ± 14.8	—	12.8 ± 7.4	77 ± 20
Model values							
Bristow-Clark model, 1982	−61	73	361	93	181	2.2	87
Irisawa-Noma model, 1982	−66	84	329	73	146	5.2	71
Noble–Noble "central" model, 1984	−61	84	263	70	147	4.7	191
Noble–Noble "peripheral" model, 1984	−73	102	254	55	122	8.1	251
Noble–DiFrancesco-Denyer model, 1989	−74	106	169	45	80	13.8	412
Model presented here	−66	97	388	91	165	7.3	80

dent "potassium background current" i_{K1} and the "pacemaker current" i_{K2}, an outward current deactivated upon hyperpolarization. This pacemaker current, however, has turned out to be an inward current activated upon hyperpolarization. The deactivation of i_{K2} can be reinterpreted as an activation of i_f (DiFrancesco, 1981), yielding a modified background potassium current $i_{b,K}$, comprising i_{K1} and the fully-activated i_{K2}. After this reinterpretation the Bristow-Clark model has the five membrane current components i_{si}, i_K, i_{Na}, and i_b. The total background current i_b consists of $i_{b,K}$ and two other background currents: $i_{b,Na}$ and $i_{b,si}$. The behavior of each of the current components during 400 ms of spontaneous electrical electrical activity is shown in Fig. 1 *A*.

The Bristow-Clark model is not useful because it does not accommodate most of the published data obtained from voltage clamp experiments. i_{K1} for instance plays a prominent role in the Bristow-Clark model whereas it experimentally appears to be nearly absent from SA node cells (Irisawa et al., 1987). The same holds true for the modification of the Bristow-Clark model by Reiner and Antzelevitch (1985). They replaced i_{K2} by an i_f current consistent with the data obtained in the first voltage clamp experiments on small SA node preparations. Further, "to generate a biologically accurate action potential," i_{K1} was increased by 30%, i_{Na} was decreased by 12% and i_{si} was increased by 15%.

Irisawa-Noma model

The Irisawa-Noma model (Irisawa and Noma, 1982) is the final form of the SA node model developed by

TABLE 2 **Electrical charge flow normalized to membrane capacitance during one cycle of spontaneous electrical activity**

	Q_{tot}	Q_{si}	Q_K	Q_f	Q_{Na}	Q_b
	mC/F	*mC/F*	*mC/F*	*mC/F*	*mC/F*	*mC/F*
Bristow-Clark model (1982)	297	103 (35%)	139 (47%)	8.6 (2.9%)	3.6 (1.2%)	44 (15%)
Irisawa-Noma model (1982)	838	360 (43%)	216 (26%)	22 (2.6%)	18 (2.2%)	222 (27%)
Noble–Noble "central" model (1984)	733	166 (23%)	366 (50%)	5.7 (0.8%)	0.9 (0.1%)	194 (27%)
Noble–Noble "peripheral" model (1984)	843	191 (23%)	420 (50%)	17 (2.1%)	1.7 (0.2%)	214 (25%)
Noble–DiFrancesco-Denyer model (1989)	1131	308 (27%)	551 (49%)	9.7 (0.9%)	3.8 (0.3%)	259 (23%)
Model presented here	908	405 (45%)	402 (44%)	35 (3.9%)	2.2 (0.2%)	64 (7.0%)

Absolute values (millicoulombs/farad) and relative values (percent of total flow).

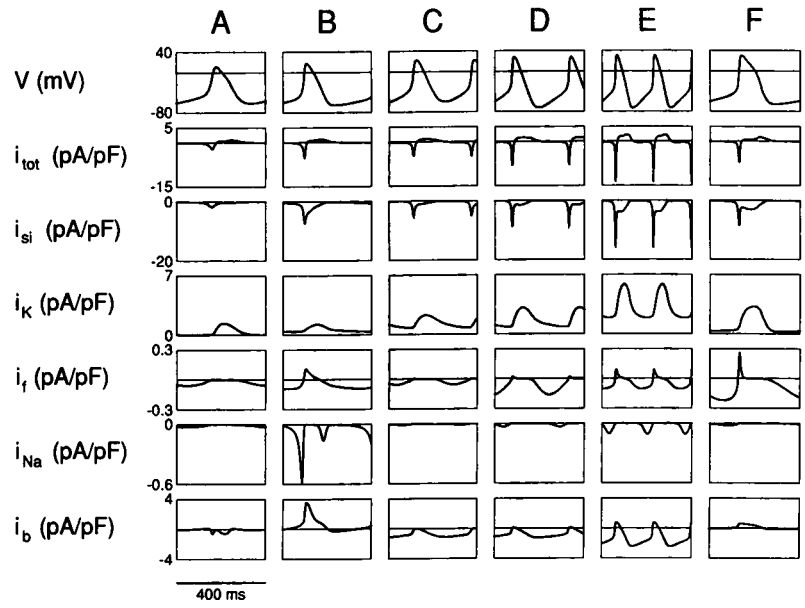

FIGURE 1 Behavior of each of the current components during 400 ms of spontaneous electrical activity. Outward currents are positive, inward currents negative. (*A*) Bristow-Clark model. (*B*) Irisawa-Noma model. (*C*) Noble–Noble "central" model. (*D*) Noble–Noble "peripheral" model. (*E*) Noble-DiFrancesco-Denyer model. (*F*) Model presented here.

Yanagihara et al. (1980). It has the same five membrane current components as the Bristow-Clark model after reinterpretation: i_{si}, i_K, i_f, i_{Na}, and i_b. The behavior of each of the current components during 400 ms of spontaneous electrical activity is shown in Fig. 1 *B*. The equations for i_{si}, i_K, and i_f are based on voltage clamp data. The i_{Na} equations were adopted from the McAllister-Noble-Tsien model (McAllister et al., 1975). The background current was estimated from the difference between the computed total amplitude of the four gated currents and the experimental steady-state current-voltage (*I-V*) curve.

The Irisawa-Noma model simulates the spontaneous electrical activity quite well (Table 1), but it has two apparent difficulties. First, the reconstruction of the experimental *I-V* curve and the action potential was satisfactory only if an artificial i_{si} "window current" was introduced by shifting the steady-state activation and inactivation curves in opposite directions. Secondly, the model has a large artificial background current (Fig. 1, Table 2).

The SA node model of Yanagihara et al., (1980) has been modified by Nilius (1986), incorporating the T-type calcium current. The $i_{Ca,T}$ equations are based on single channel and whole cell currents recorded from guinea pig ventricular and atrial cells, respectively. Unlike the model by Yanagihara et al., (1980) no artificial window current was needed to evoke pacemaker activity. Comparing the $d_{T,\infty}$- and $f_{T,\infty}$-curves of Nilius (1986) to those of Hagiwara et al. (1988), who carried out experiments on single rabbit SA node cells, shows that, unfortunately, the artificial i_{si} window current was replaced by a large artificial $i_{Ca,T}$ window current: in contrast to the $d_{T,\infty}$- and $f_{T,\infty}$-curves of Nilius (1986) the curves of Hagiwara et al. (1988) hardly overlap (Fig. 3, left panel).

Noble-Noble model

The Noble–Noble model (Noble and Noble, 1984) is a modification of the DiFrancesco-Noble model (DiFrancesco and Noble, 1985). The membrane current components of this cardiac Purkinje fibre model were modified for the SA node. The same equations were used with parameters appropriate to the SA node except where specific information on the SA node existed that required the equations to be changed.

The model incorporates i_{NaCa} and i_{NaK} and accounts for the variations in ion concentrations. i_{si} is separated into fast gated component $i_{Ca,f}$ and i_{NaCa}. The $i_{Ca,f}$ equations incorporate calcium-dependent inactivation. The equations for i_f and i_K are based on voltage clamp experiments on multicellular SA node preparations. The i_{Na} equations are based on data obtained on Purkinje fibers. The equations for i_{NaCa} and for intracellular calcium storage and release are only partly based on experimental

observations. The conductance $g_{b,Ca}$ of the calcium background current $i_{b,Ca}$ was chosen to give a diastolic free calcium level in the presumed physiological range of 50–100 nM. The maximum value for the conductance g_{K1} of the potassium background current i_{K1} was reduced to a small arbitrary value. The conductance $g_{b,Na}$ of the sodium background current $i_{b,Na}$ was chosen as that which allowed a MDP between ~ -70 and -55 mV to be achieved. The equation for i_{NaK} was chosen to allow the intracellular sodium and potassium concentrations to be maintained during spontaneous electrical activity.

The "central" version of the model differs from the standard "peripheral" version in that the $\bar{i}_{Ca,f}$ and $\bar{i}_K$ are reduced by 37.5 and 33%, respectively. The behavior of each of the current components of both the central and the peripheral version during 400 ms of spontaneous electrical activity is shown in Fig. 1, *C* and *D*. The total background current i_b consists of $i_{b,Ca}$, i_{K1}, $i_{b,Na}$, and i_{NaK}. Both versions simulate the spontaneous electrical activity to a quite reasonable degree (Table 1).

The major difficulties for our purposes lie in the fact that not all model quantities, if simply scaled down by a factor of 100 as explained before, resemble the single cell experimental data. First, the thus obtained value of the membrane capacitance (60 pF) is very large compared with the experimentally observed values (Table 3). Secondly, the thus obtained value of the cell volume (14,469 μm^3), related to the action potential through the intracellular ion concentrations, is very large compared with the values that can be inferred from the experimentally observed cell dimensions (see below). Thirdly, under voltage clamp conditions the kinetics of i_{si}, i_f, and i_K do not agree with the data obtained from experiments on single SA node cells (not shown).

TABLE 3 Capacitance of isolated rabbit SA node cells

	C
	pF
DiFrancesco, 1986 (mean ± SD, $n = 20$)	29.3 ± 9.5
Irisawa et al., 1987 (mean ± SD, $n = 18$)	29.2 ± 11
Irisawa and Hagiwara, 1988 (range)	30 to 40
Hagiwara et al., 1988 (mean ± SD, $n = 26$)	35.4 ± 4.8
Belardinelli et al., 1988 (mean ± SD, $n = 18$)	35.4 ± 7.7
Denyer and Brown, 1990*a* (mean ± SD, $n = 26$)	28.3 ± 13.3

Noble-DiFrancesco-Denyer single cell model

The Noble-DiFrancesco-Denyer single cell model (Noble et al., 1989) is a modification of the Noble–Noble peripheral model (Noble and Noble, 1984). Comparing current magnitudes in the multicellular model with experimentally observed single cell current magnitudes suggested that the multicellular preparation had included ~ 100 cells. Therefore, all membrane ionic currents were scaled down by a factor of 100. The single cell was assumed to be a cylinder of 100 μm in length and 8 μm in diameter having a capacitance of 27 pF (Denyer, 1989). The equations for i_f and i_K were replaced by equations based on more recent single cell experimental data (DiFrancesco and Noble, 1989). The equation for $\bar{i}_K$, however, had to be scaled up by a factor of 2.7 to evoke pacemaker activity. The behavior of each of the current components of the thus obtained single cell model during 400 ms of spontaneous electrical activity is shown in Fig. 1 *E*.

The Noble-DiFrancesco-Denyer model has the following drawbacks:
(*a*) Many of the computed values of the action potential parameters differ largely from the experimentally observed values (Table 1). (*b*) As mentioned before the value of $\bar{i}_K$ does not correspond to the experimental findings. (*c*) Due to the overestimation of $\bar{i}_K$ the sodium-potassium pump current i_{NaK} and the background sodium current $i_{b,Na}$ are probably overestimated too because the magnitude of i_{NaK} is linked to the efflux of potassium through the i_K channels and the magnitude of $i_{b,Na}$ in turn is linked to the efflux of sodium ions through the sodium-potassium pump. (*d*) Due to the large values of other currents and the short CL the contribution of i_f is probably underestimated (Table 2). (*e*) A common finding in voltage clamp records is that at holding potentials from -40 to -30 mV the amplitude of the background current is <10 pA (Irisawa et al., 1991). In the model however it is 40 pA. (*f*) The model does not incorporate the T-type calcium current.

A NEW SINGLE CELL MODEL

In this section we present and discuss the parameters and equations of our single cell model. Single cell experimental data on the cell dimensions, the membrane capacitance, and the currents $i_{Ca,L}$, $i_{Ca,T}$, i_f, i_K, and i_{NaK} were used to construct the model. If sufficient data were not available, which was the case with the intracellular calcium uptake and release processes, and the currents $i_{b,Ca}$, $i_{b,Na}$, and i_{NaCa}, the model equations were

adopted from the Noble-Noble model (Noble and Noble, 1984).

Dimensions and capacitance of the model cell

There is a wide variety in the cellular morphology of cells isolated from the SA node region (Denyer and Brown, 1990*a*; van Ginneken and Giles, 1991). The SA node cells used in voltage clamp experiments, however, mostly are elongated, spindle-shaped cells. Irisawa et al. (1987) used spindle-shaped cells with a length of 112 ± 40 μm and a width of 9 ± 5 μm (mean ± SD, $n = 93$). Denyer and Brown (1990*a*) also used spindle-shaped cells. They report a length of 95 ± 34 μm (mean ± SD, $n = 39$) and a width of 7.1 ± 0.6 μm (mean ± SD, $n = 9$). As an average we assumed our model cell to be a 100 μm long by 8 μm diameter cylinder, the same dimensions as in the Noble-DiFrancesco-Denyer model. So our model cell has a membrane area of 2,613.8 μm^2 and a volume of 5,026.5 μm^3. The calculated action potential does not depend strongly on the cell volume.

As an average of the reported capacitance values (Table 3) we set the cell capacitance to 32 pF. This gives a value of 1.22 $\mu F/cm^2$ for the membrane capacitance normalized to the calculated membrane area, agreeing well with the experimental value of 1.30 ± 0.24 $\mu F/cm^2$ (mean ± SD, $n = 18$) obtained by Nakayama et al. (1984).

Ion concentrations

We assumed the extracellular concentrations of calcium, potassium, and sodium ions to be 2.0, 5.4, and 140 mM, respectively. These are the usual values for the bathing solutions in single cell experiments. We required the intracellular concentrations of potassium and sodium ions to maintain their assumed values of 140 and 7.5 mM, respectively (Noble and Noble, 1984) during a long period of spontaneous electrical activity. The variations of these values during one cycle of pacemaker activity, calculated from Eqs. 21 and 22, are very small. The variation of the intracellular concentration of free calcium ions is calculated from Eq. 20. This concentration varies from 66 nM to 10 μM during one cycle of pacemaker activity. This variation is within the range expected from experimental measurements and model studies on the intracellular free calcium concentration (Chapman and Noble, 1989).

Calcium storage and release

The intracellular calcium uptake and release processes are described by the equations given by Noble and Noble (1984) which represent the electrophysiologically essential features of these complex processes.

Time-dependent (gated) currents

L-type calcium current ($i_{Ca,L}$)

After Hagiwara et al. (1988), who studied the kinetic properties of $i_{Ca,L}$ and $i_{Ca,T}$ in single rabbit SA node cells, the kinetics of $i_{Ca,L}$ are described with an activation gating variable d_L and an inactivation gating variable f_L. We used their Eqs. 1 and 2 to describe the steady-state activation and inactivation.

No quantitative single cell experimental data are available on the very fast activation of $i_{Ca,L}$. Assuming voltage dependence only, one would expect the time constant of inactivation, i.e., the decrease in f_L, to be the same as that of recovery from inactivation, i.e., the increase in f_L. This time constant, however, seems to depend on the degree of inactivation: experimental findings suggest that it varies from ~4 ms at $f_L = 1$ to 225 ms at $f_L = 0$. The value of 4 ms can be calculated from Fig. 6 *B* of Nakayama et al. (1984) which shows the inactivation time course at 10 mV. The value of 225 ms is the time constant of recovery from inactivation measured at −40 mV by Hagiwara et al. (1988): they report a value of 225 ± 12.5 ms (mean ± SD, $n = 3$). We have chosen Eqs. 3 and 4 to describe the $i_{Ca,L}$ time constants. These equations fit the above mentioned experimental data and yield voltage clamp results which agree well with the experimental findings of DiFrancesco et al. (1986) and DiFrancesco and Noble (1989) (Fig. 2 *C*).

We adopted the Noble–Noble equation for $i_{Ca,f}$, which accounts for the dependence on the membrane potential

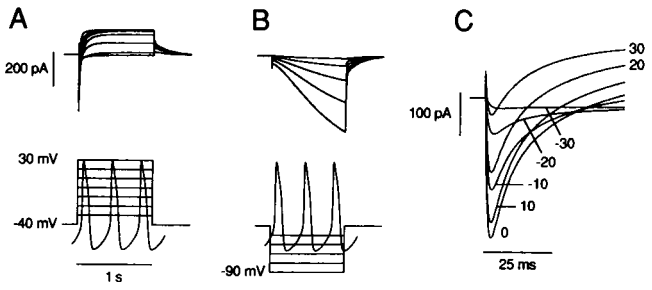

FIGURE 2 Computed voltage clamp records. The upper panels of *A* and *B* show superimposed records of the total membrane current in response to 1 s voltage clamp pulses from a holding potential of −40 mV. Voltage clamp pulses superimposed on the spontaneous electrical activity of the model cell are shown in the lower panels. (*A*) Activation of i_{si} and i_K upon depolarizing steps to test potentials ranging from −30 to 30 mV. (*B*) Activation of i_f upon hyperpolarizing steps to test potentials ranging from −50 to −90 mV. (*C*) Current traces of *A* on an expanded time scale, showing the activation of i_{si}. Test potentials indicated near corresponding traces.

and the intracellular free calcium concentration, to describe $\bar{i}_{Ca,L}$. The maximum amplitude of i_{si}, measured in voltage clamp experiments as the difference between the peak of i_{si} and the current level 200 ms after the onset of the voltage clamp step, is attained near 0 mV and ranges from 9 to 37 $\mu A/cm^2$ with an average of 16.9 ± 6.8 $\mu A/cm^2$ (mean ± SD, $n = 8$) (Nakayama et al., 1984). Thus, for our model cell with a membrane area of 2,613.8 μm^2 one should have a maximum i_{si} amplitude of 442 pA. In the model, it is 444 pA attained at 2 mV. This has been achieved by setting $P_{Ca,L}$ to 90 pA/mM.

T-type calcium current ($i_{Ca,T}$)

No experimental data are available on the dependence of $i_{Ca,T}$ on the intracellular free calcium concentration $[Ca^{2+}]_i$. Experimental results indicate that $\bar{i}_{Ca,T}$ shows about the same dependence on the extracellular calcium concentration and the membrane potential as $\bar{i}_{Ca,L,Ca}$ (Hagiwara et al., 1988). Therefore, we have chosen Eq. 9 for $\bar{i}_{Ca,T}$ to be of the same form as the equation for $\bar{i}_{Ca,L,Ca}$.

According to the experimental results of Hagiwara et al. (1988) the kinetics of $i_{Ca,T}$ are described with an activation gating variable d_T and an inactivation gating variable f_T. The steady-state activation and inactivation are described by their Eqs. 5 and 6 (Fig. 3, left panel). Eq. 8 for the time constant of inactivation has been determined by fitting the experimental data Fig. 9 *C* of Hagiwara et al. (1988) (Fig. 3, middle panel). No quantitative data are available on the very small time constant of activation. Using $P_{Ca,T} = 85$ pA/mM and Eq. 7, we obtained model voltage clamp results similar to Figs. 1 *C* and 8 *A1* of Hagiwara et al. (1988) (Fig. 3, right panel).

Hyperpolarizing-activated current (i_f)

The i_f channels are permeable to both sodium and potassium ions. The experimentally observed $\bar{i}_f$ current-voltage relation is approximately linear and the reversal potential lies somewhere between the potassium equilibrium potential and the sodium equilibrium potential (DiFrancesco et al., 1986; van Ginneken and Giles, 1991). Therefore, we have chosen Eq. 13 to describe $\bar{i}_f$. van Ginneken and Giles report an i_f reversal potential of −24 ± 4 mV (mean ± SD, $n = 6$) and a maximum i_f conductance of 12 ± 3.6 nS (mean ± SD, $n = 17$). Model values of −24 mV and 12 nS are achieved by setting $g_{f,K} = 7.4$ nS and $g_{f,Na} = 4.6$ nS.

The experimental data on the i_f kinetics can be fitted well by assuming the presence of two identical gates (Denyer, 1989; van Ginneken and Giles, 1991). Therefore, we have chosen Eq. 13 to describe i_f. We have adopted Eqs. 11 and 12 of van Ginneken and Giles (1991) for the rate constants.

Model voltage clamp results (Fig. 2 *B*) agree well with the experimental results of DiFrancesco et al. (1986), Denyer and Brown (1990*b*), and van Ginneken and Giles (1991).

Delayed rectifying potassium current (i_K)

Carrying out experiments on cells isolated from rabbit SA and atrioventricular (AV) nodes, which, in the case of i_K, were not distinguished, Nakayama et al. (1984) found a nonlinear $\bar{i}_K - V$ relationship with a reversal potential obtained between −75 and −65 mV and a peak amplitude of ~4 $\mu A/cm^2$ attained between −10 and 20 mV in five examples. For our model cell with a membrane area of 2,613.8 μm^2 this peak amplitude should be 105 pA. We fit these experimental data by Eq. 16 with the scaling factor k_K set to 11. This yields a $\bar{i}_K - V$ relationship with a reversal potential of −70 mV and a peak amplitude of 111 pA attained at 6.5 mV (Fig. 4). Shibasaki (1987) studied the i_K kinetics of single rabbit SA and AV node cells, which, too, were not distinguished. It was shown that a fast inactivation gate can be responsible for the observed nonlinearity of $\bar{i}_K$, known as "inward-going rectification." We did not incorporate this gate into our model because the data only refer to potentials negative to −50 mV. So the time-dependence

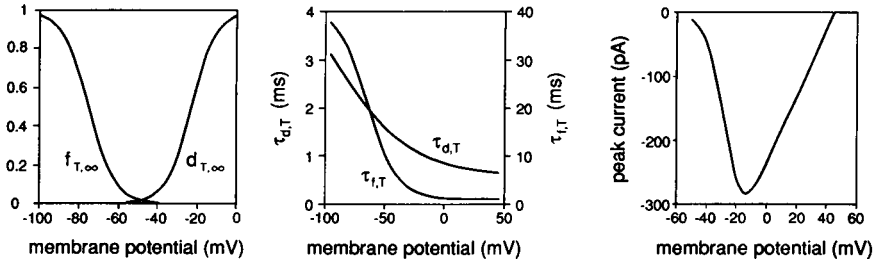

FIGURE 3 Computed characteristics of the T-type calcium current. (*Left*) Steady-state activation ($d_{T,\infty}$) and steady-state inactivation ($f_{T,\infty}$). (*Middle*) Time constant of activation ($\tau_{d,T}$) and time constant of inactivation ($\tau_{f,T}$); note different ordinate scales. (*Right*) Peak current in response to voltage clamp steps from −80 mV to various test potentials from −50 to +45 mV. Curves drawn according to Eqs. 5–9.

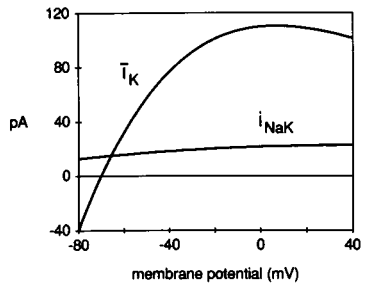

FIGURE 4 Fully-activated delayed rectifying potassium current as a function of the membrane potential ($\bar{i}_K$). Sodium-potassium pump current as a function of the membrane potential at an intracellular sodium concentration of 7.5 mM (i_{NaK}). Curves drawn according to Eqs. 16 and 17.

is described by one gating variable only: the activation gating variable x. We used Shibasaki's (1987) Eqs. 14 and 15 for the steady-state activation and the time constant of activation. Model voltage clamp results (Fig. 2*A*) agree well with the experimental results of Nakayama et al. (1984), DiFrancesco et al. (1986), and Shibasaki (1987).

Fast sodium current (I_{Na})

Experimental results on the presence of i_{Na} in SA node cells, indicated by their sensitivity to tetrodotoxin (TTX), are largely different: in some studies i_{Na} was nearly always present (Oei et al., 1989; Denyer and Brown, 1990*a*), whereas in others it appeared to be completely absent (van Ginneken and Giles, 1991). For completeness, we have incorporated a small i_{Na} into our model. Because no quantitative data are available on this current in SA node cells we have adopted the Noble–Noble i_{Na} equations, scaled down properly, which are based on single cell experiments on Purkinje fibres. According to these equations the i_{Na} channel is to some extent permeable to potassium ions. The amount of i_{Na} carried by potassium is so small that we have neglected it in the equations for $i_{K,net}$ and $i_{Na,net}$.

Pump and exchange currents

Sodium-calcium exchange current (I_{NaCa})

We have adopted the Noble–Noble i_{NaCa} equation with the scaling factor k_{NaCa} reduced by a factor of 200 to 0.01. Using an intracellular perfusion method Hagiwara and Irisawa (1988) observed an i_{NaCa} current density of 1 pA/pF at a membrane potential of −40 mV and an intracellular free calcium concentration of 500 nM. Our model equation yields a value of 0.64 pA/pF.

Sodium-potassium pump current (I_{NaK})

No experimental data are available on the voltage dependence or the amplitude of i_{NaK} in SA node cells. In isolated guinea pig ventricular cells, however, Gadsby et al. (1985) found a marked voltage dependence and an amplitude of 3 ± 1 μA/cm² (mean ± SD, n = 9) at an intracellular sodium concentration $[Na^+]_i$ of 34 mM. Assuming that i_{NaK} in SA node cells shows the same voltage dependence we obtained in Eq. 17. The factor describing the dependence on $[Na^+]_i$, with a $K_{m,Na}$ value of 40 mM, was adopted from the Noble–Noble model. We set $i_{NaK,max}$, the "maximum" Na-K pump current, to 182 pA. This value was found by varying $i_{NaK,max}$ and the background sodium conductance until the intracellular sodium and potassium concentrations were maintained during long runs, i.e., several hundreds of action potentials, of pacemaker activity. With this value the computed amplitude of i_{NaK} at $[Na^+]_i$ = 34 mM is 3.2 μA/cm².

The voltage dependence of i_{NaK} is depicted in Fig. 4. The average value of i_{NaK} during one cycle of pacemaker activity is 24.1 pA or 0.75 pA/pF, the peak value 28.7 pA or 0.90 pA/pF.

Time-independent (background) currents

Background calcium current ($I_{b,Ca}$)

The inward background calcium current is described by the Noble–Noble Eq. 18. This current is needed to keep the diastolic level of the intracellular free calcium concentration in the generally accepted range of 60–100 nM (Chapman and Noble, 1989). A $g_{b,Ca}$ value of 0.04 nS is sufficient to achieve this. The average value of $i_{b,Ca}$ during one cycle of pacemaker activity is 6.3 pA or 0.20 pA/pF, the peak value 8.1 pA or 0.25 pA/pF.

Background potassium current ($I_{b,K}$)

In single channel experiments on rabbit SA node cells a small amount of i_{K1} channels was found (Irisawa et al., 1987). These channels account for a small outward background current $i_{b,K}$. We adopted the Noble–Noble i_{K1} equations, scaled down by a factor of 100, to describe this current. The average value of $i_{b,K}$ during one cycle of pacemaker activity is 2.8 pA or 0.09 pA/pF, the peak value 4.9 pA or 0.15 pA/pF.

Background sodium current ($I_{b,Na}$)

The inward background sodium current is described by the Noble–Noble Eq. 19. Our value of 0.15 nS for $g_{b,Na}$ was determined together with $i_{NaK,max}$ in the way described before. The average value of $i_{b,Na}$ during one cycle of pacemaker activity is 17.7 pA or 0.55 pA/pF, the peak value 21.6 pA or 0.67 pA/pF.

RESULTS AND DISCUSSION

A large part of the discussion has already been presented in previous sections. Hence, we will restrict ourselves to a more general discussion in this section.

Heterogeneity of SA node cells

There is a large variation in the action potential parameters of the rabbit SA node cells used in different studies (Table 1). Voltage clamp results, too, lie within a wide range. In the case of i_f, it is still in doubt whether this current is consistently present: in some studies i_f was only found in a part of the cells (Nakayama et al., 1984; DiFrancesco et al., 1986), whereas in others it was always present (Denyer and Brown, 1990*a*; van Ginneken and Giles, 1991). As mentioned before, i_{Na} is not consistently found too. Some variations may arise from differences in isolation methods or recording techniques. However, large variations are also reported within series of similar experiments. For example, the amplitude of i_{si} ranges from 9 to 37 $\mu A/cm^2$ in the experiments of Nakayama et al. (1984). Similarly, the size and kinetics of i_f are variable to ±30% in the experiments of van Ginneken and Giles (1991). Thus, it is likely that isolated SA node cells exhibit a high degree of heterogeneity in their electrophysiological properties. One may hypothesize that this reflects the regional differences in action potential parameters in the intact SA node (Bleeker et al., 1980; op 't Hof et al., 1987). It is not at all clear whether the heterogeneity is mainly based on a large variability in ion channel densities or that intracellular factors are largely involved. Anyway, the creator of the model is faced with a fundamental problem: each cell requires its own model and two cells may require essentially different models. Only if a complete set of voltage clamp data recorded from one cell were available to the creator of the model, it might be possible to construct an accurate model of this one cell. At present, the best thing the creator of a model can do is to use the average values obtained in voltage clamp experiments, hoping that cells with these average values exist and are not infrequent.

Voltage clamp experiments

The results of the application of all "standard" voltage clamp protocols to our model cell are depicted in Fig. 2. As already discussed before the experimental data are reproduced well. The activation of the slow inward current (Fig. 2 *C*) could not be reproduced well by any of the other models (not shown).

Plotting the total membrane current as a function of the applied test potential we obtain the I-V relationship of our model cell (Fig. 5). Hyperpolarizing pulses near −50 mV clearly elicit a positive shift in current after 5 ms, corresponding to the experimental results of Denyer (1989) and van Ginneken and Giles (1991). Other aspects of this relationship also fit the experimentally found *I-V* relationships (Nakayama et al., 1984; Irisawa and Hagiwara, 1988; Denyer and Brown, 1990*a*; van Ginneken and Giles, 1991).

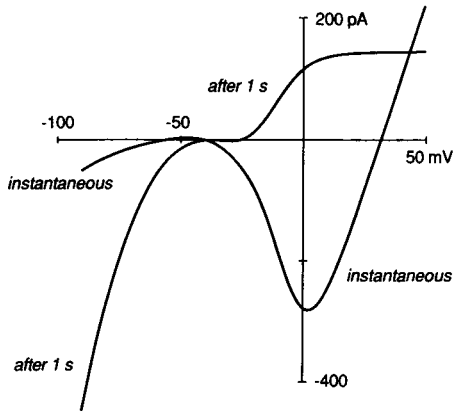

FIGURE 5 Current-voltage relationship for the total membrane current of the model cell at the end of 5 ms or 1 s voltage clamp pulses from a holding potential of −40 mV.

As mentioned before the amplitude of the background current at holding potentials from −40 to −30 mV is commonly found to be <10 pA (Irisawa et al., 1991). In our model cell it is <3 pA.

Spontaneous electrical activity

The behavior of the membrane potential and all 10 membrane current components during pacemaker activity is depicted in Fig. 6, clearly showing the relative contribution of each component in generating the action potential. The currents $i_{Ca,L}$, $i_{Ca,T}$, and i_{NaCa} as well as the currents $i_{b,Ca}$, $i_{b,K}$, $i_{b,Na}$, and i_{NaK}, added up to give i_{si} and i_b, respectively, in Fig. 1 *F*, are shown separately now. Our model $i_{Ca,L}$ is very similar to the $i_{Ca,L}$ obtained by Doerr et al. (1989) during "action potential clamp" of a single rabbit SA node cell. Their $i_{Ca,T}$ during diastolic depolarization, however, is considerably larger than our model $i_{Ca,T}$. The latter fact, as well as the contribution of i_f and i_b to the slow diastolic depolarization phase, will be discussed in detail below.

The action potential parameters of our model cell are listed in Table 1. It should be stressed that we did not use the experimentally observed values of action potential parameters, except the APA values as we will discuss

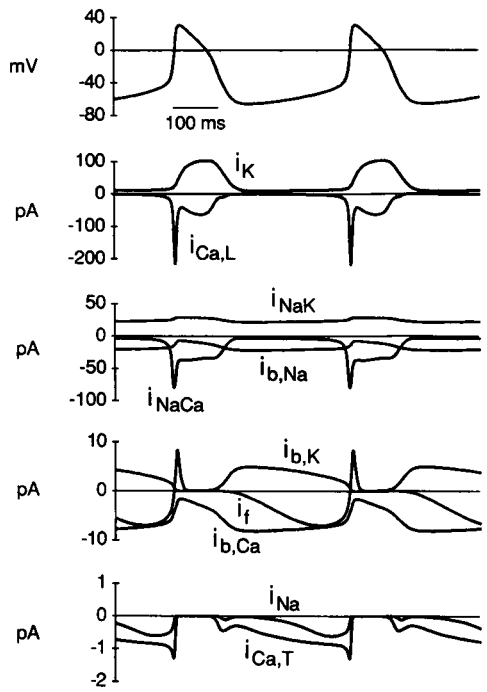

FIGURE 6 Behavior of all membrane current components of the model cell during spontaneous electrical activity. Note differences in current scales.

below, in selecting model equations or model parameters.

Determination of model parameters

Unfortunately, in constructing our model we had to combine the experimental data obtained in different studies. Nevertheless, it was possible to construct a satisfactory model without setting the scaling parameters determining the magnitude of the membrane current components to unreasonable values. In fact the scaling parameters for $i_{Ca,L}$, $i_{Ca,T}$, i_f, and i_K were selected to yield the average values of experimentally found current magnitudes. The scaling parameters of i_{Na} and $i_{b,K}$ had to be set to arbitrary values because no quantitative experimental data were available on the i_{Na} and $i_{b,K}$ magnitudes in SA node cells. The values of the scaling parameters for $i_{b,Ca}$, $i_{b,Na}$, and i_{NaK} were determined by examining the variation of the intracellular ion concentrations. The main effect of an increase (decrease) in the scaling parameter k_{NaCa} for i_{NaCa} is an increase (decrease) in the overshoot of the action potential and hence in the action potential amplitude APA. Setting k_{NaCa} to 0.01 resulted in a satisfactory APA.

Although during pacemaker activity $i_{b,Ca}$, $i_{b,K}$, i_{Na}, and i_{NaK} have average values (peak values) ranging from 2.8 pA or 0.09 pA/pF (4.9 pA or 0.15 pA/pF) to 24.1 pA or 0.75 pA/pF (28.7 pA or 0.90 pA/pF) the net current resulting from these four currents does not exceed 20 pA or 0.63 pA/pF. In fact the average value (peak value) of this net current is only 5.4 pA or 0.17 pA/pF (20.0 pA or 0.62 pA/pF, attained during the overshoot of the action potential). In this respect our model differs radically from the Noble-DiFrancesco-Denyer model, in which the average value (peak value) of this net current is 41.3 pA or 1.53 pA/pF (66.0 pA or 2.44 pA/pF).

Inactivation of $i_{Ca,L}$

An essential feature of our model is the dependence of the $i_{Ca,L}$ time constant of inactivation, $\tau_{f,L}$, on the inactivation gating variable f_L. It is likely that this dependence reflects some inactivation process triggered by the influx of calcium ions preceding the decrease in f_L. Rather than making assumptions on this process, or combination of processes, we directly incorporated this marked dependence into our model.

The dependence of $\tau_{f,L}$ on f_L causes $i_{Ca,L}$ to be largely inactivated during the repolarization phase of the action potential. In the DiFrancesco-Noble model as well as in the Noble–Noble model, and the Noble-DiFrancesco-Denyer model, in which $\tau_{f,L}$ has a nearly constant value of 20 ms, this could only be achieved by incorporating a second inactivation gating variable representing an inactivation process depending on the free intracellular calcium concentration. This gating variable f_2, however, is not enough to prevent $i_{Ca,L}$ from being partly activated during the repolarization phase of the action potential. The large i_K in the Noble-DiFrancesco-Denyer model causes this activation to be masked in two ways. The inward current generated by $i_{Ca,L}$ during repolarization is more than compensated by the large i_K. Furthermore the action potential duration APD_{50} is so short (Table 1) that the recovery from the f_2-inactivation is far from complete at 50% repolarization. If i_K is scaled down according to the experimental data pacemaker activity ceases due to the activation of $i_{Ca,L}$ during repolarization.

Effect of EGTA buffering

In most experimental studies EGTA was added to the recording pipette solution resulting in buffering the free intracellular calcium concentration $[Ca^{2+}]_i$. If necessary, e.g., in our model voltage clamp experiments, we simulated EGTA buffering by fixing $[Ca^{2+}]_i$ to 80 nM. One should be aware of this because activation of the sodium-calcium exchanger significantly alters the voltage clamp records and hence the current voltage relationship: without EGTA buffering the magnitude of the

inward peak current in the instantaneous current-voltage relationship increases by 18%.

Role of i_f and i_b

The inward current generated by i_f contributes significantly to the net current during slow diastolic depolarization. The effect of selectively and completely blocking i_f on the model action potential is depicted in Fig. 7. The model effect resembles the experimentally observed effect (Denyer and Brown, 1990*b*; van Ginneken and Giles, 1991). Blocking i_f in the model cell yields a 16% decrease in beating rate, greater than in other models with about the same i_f equations (Table 4). A value of 19% (n = 3) was found in patched SA node cells where i_f was selectively and completely blocked by 2 mM Cs^+ (Denyer and Brown, 1990*b*). In unpatched cells, where no inward seal leak current can contribute to the diastolic depolarization, they found a slowing of 30% (n = 13). This suggests that in our model i_b, generating a net inward current during diastolic depolarization, is still overestimated, although it has been greatly reduced compared with other models (Fig. 1, Table 2). This can be due to an overestimation of $g_{b,Na}$. The intracellular sodium concentration is maintained using a $g_{b,Na}$ value of 0.15 nS. A lower value could be sufficient if other mechanisms raising the intracellular sodium concentration, e.g., the Na-H exchanger, are taken into account. At the moment, however, no useful quantitative data are available on the Na-H exchanger in cardiac cells.

To investigate the effects of reducing i_b we performed some calculations with $g_{b,Na}$ reduced by 20% to 0.12 nS. This reduction hardly affected the shape of the action potential (not shown) and the main effect was seen during the diastolic depolarization. Due to the reduction of $g_{b,Na}$ the membrane potential reaches a MDP, which is more negative by 2 mV. As this MDP is closer to the i_K reversal potential the outward current carried by i_K decreases. This decrease in outward current is nearly balanced by a net decrease in inward current as can be inferred from the net membrane current i_{tot} being almost

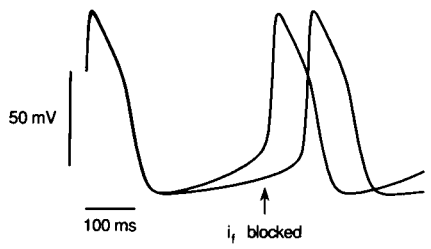

FIGURE 7 Effect of blocking i_f on the spontaneous electrical activity of the model cell.

TABLE 4 **Slowing of spontaneous activity due to block of i_f**

	Cycle length		Slowing of beating rate
	Normal	i_f Blocked	
	ms	*ms*	
Bristow-Clark model (1982)	361	438	17%
Irisawa-Noma model (1982)	329	364	10%
Noble-Noble "central" model (1984)	263	270	3%
Noble-Noble "peripheral" model (1984)	254	268	5%
Noble-DiFrancesco-Denyer model (1989)	169	173	2%
Model presented here	388	461	16%

unchanged. This net decrease in inward current results from an increase in i_f, which is more activated at more negative membrane potentials, and a net decrease in the remaining currents of which only $i_{b,Na}$ is changed significantly. In summary: the contribution of i_f to i_{tot} increases upon a 20% reduction of $g_{b,Na}$. Consequently, blocking i_f yields a greater slowing in beating rate: 25%, closer to the experimentally observed value of 30%.

One may argue that the block of i_f turns i_{tot} from an inward current into an outward current because i_f is greater in magnitude than i_{tot} during the slow diastolic depolarization phase of the action potential (not shown). Our model cell, however, preserves its slow diastolic depolarization upon blocking i_f: the i_K decay, which normally stops within 20 ms after reaching the MDP, continues for more than 200 ms after reaching the MDP, thereby keeping i_{tot} from turning into an outward current.

The question to which extent an inward background current, probably carried by sodium ions (Irisawa et al., 1991), contributes to the slow diastolic depolarization, normally or after blocking i_f, has been addressed by both theoretical and experimental workers. The attempts to answer this question by simple, partial modeling of the diastolic depolarization (DiFrancesco and Noble, 1989; Noble et al., 1989) have left the issue open. From experimental work it was concluded that an inward background current must exist since pacemaker activity continues after blocking i_f effectively and selectivity (Brown and Denyer, 1990; Denyer and Brown, 1990*b*). Moreover, pacemaker activity was also found in cells lacking i_f activation within the pacemaker potential range (Nathan, 1987).

Our model cell still shows pacemaker activity upon a complete removal of $i_{b,Na}$. However, it turns quiescent if subsequently i_f is blocked. This model result supports the conclusion drawn by Nathan as well as Denyer and

Brown that an inward background current contributes substantially to the slow diastolic depolarization of the action potential. The overall conclusion from our model results is that during normal pacemaker activity the slow diastolic depolarization is generated mainly by i_f and this inward background current.

Role of $i_{Ca,T}$

Electrophysiologists do not agree on the extent to which $i_{Ca,T}$ contributes to the generation of the action potential. Our $i_{Ca,T}$ equations, which resemble the experimental data obtained in voltage clamp experiments, yield an $i_{Ca,T}$ amplitude during pacemaker activity which is <1.5 pA or 0.05 pA/pF (Fig. 6). Thus, $i_{Ca,T}$ does not play an important role in the normal pacemaker activity of our model cell. Blocking it causes a slowing in beating rate of only 2.0%, in agreement with the experimental findings in our laboratory that blocking $i_{Ca,T}$ with 50 μM Ni^{2+} hardly affects the cycle length of rabbit SA node cells (Verheijck, E.E., and L.N. Bouman, unpublished observations). As mentioned before, the cells of Doerr et al. (1989) show a considerably larger $i_{Ca,T}$, which explains the larger effect of 40 μM Ni^{2+} on beating rate found in their experiments.

APPENDIX

Currents and concentrations

Membrane potential

$$dV/dt = -i_{tot}/C$$

$$i_{tot} = i_{b,Ca} + i_{b,K} + i_{b,Na} + i_{Ca,L} + i_{Ca,T} + i_f + i_K + i_{Na} + i_{NaCa} + i_{NaK}$$

L-type calcium current ($i_{Ca,L}$)

$$i_{Ca,L} = d_L f_L(\bar{i}_{Ca,L,Ca} + \bar{i}_{Ca,L,K} + \bar{i}_{Ca,L,Na})$$

$$d_{L,\infty} = 1/\{1 + \exp[-(V + 6.6)/6.6]\} \quad (1)$$

$$f_{L,\infty} = 1/\{1 + \exp[(V + 25)/6]\} \quad (2)$$

$$\tau_{d,L} = 2 \quad (3)$$

$$\tau_{f,L} = 4 + 2.21[(1 - f_L)/(0.1 + f_L)]^2 \quad (4)$$

$$\bar{i}_{Ca,L,Ca} = 2P_{Ca,L}([(V - 50)/(RT/2F)]/\{1 - \exp[-(V - 50)/(RT/2F)]\}) \cdot \{[Ca^{2+}]_i \cdot \exp[50/(RT/2F)] - [Ca^{2+}]_e \exp[-(V - 50)/(RT/2F)]\}$$

$$\bar{i}_{Ca,L,K} = P_{Ca,L,K}P_{Ca,L}([(V - 50)/(RT/F)]/\{1 - \exp[-(V - 50)/(RT/F)]\}) \cdot \{[K^+]_i \exp[50/(RT/F)] - [K^+]_e \exp[-(V - 50)/(RT/F)]\}$$

$$\bar{i}_{Ca,L,Na} = P_{Ca,L,Na}P_{Ca,L}([(V - 50)/(RT/F)]/\{1 - \exp[-(V - 50)/(RT/F)]\})\{[Na^+]_i \cdot \exp[50/(RT/F)] - [Na^+]_e \exp[-(V - 50)/(RT/F)]\}$$

T-type calcium current ($i_{Ca,T}$)

$$i_{Ca,T} = d_T f_T \bar{i}_{Ca,T}$$

$$d_{T,\infty} = 1/\{1 + \exp[-(V + 23)/6.1]\} \quad (5)$$

$$f_{T,\infty} = 1/\{1 + \exp[(V + 75)/6.6]\} \quad (6)$$

$$\tau_{d,T} = 0.6 + 5.4/\{1 + \exp[0.03(V + 100)]\} \quad (7)$$

$$\tau_{f,T} = 1 + 40/\{1 + \exp[0.08(V + 65)]\} \quad (8)$$

$$\bar{i}_{Ca,T} = 2P_{Ca,T}([(V - 50)/(RT/2F)]/\{1 - \exp[-(V - 50)/(RT/2F)]\})\{[Ca^{2+}]_i \cdot \exp[50/(RT/2F)] - [Ca^{2+}]_e \exp[-(V - 50)/(RT/2F)]\} \quad (9)$$

Hyperpolarizing-activated current (i_f)

$$i_f = y^2 \bar{i}_f \quad (10)$$

$$\alpha_y = \exp[-0.0220741(V + 386.9)] \quad (11)$$

$$\beta_y = \exp[0.052(V - 73.08)] \quad (12)$$

$$\bar{i}_f = g_{f,K}(V - V_K) + g_{f,Na}(V - V_{Na}) \quad (13)$$

$$V_K = (RT/F)\log([K^+]_e/[K^+]_i)$$

$$V_{Na} = (RT/F)\log([Na^+]_e/[Na^+]_i)$$

Delayed rectifying potassium current (i_K)

$$i_K = x\bar{i}_K$$

$$x_\infty = 1/(1 + \exp[(V + 25.1)/7.4]) \quad (14)$$

$$\tau_x = 1/[0.017\exp(0.0398V) + 0.000211\exp(-0.051V)] \quad (15)$$

$$\bar{i}_K = k_K(V + 70)/[1 + 6\exp(0.015V)] \quad (16)$$

Fast sodium current (i_{Na})

$$i_{Na} = m^3 h g_{Na}(V - V_{Na,K})$$

$$\alpha_h = 0.02\exp[-0.125(V + 75)]$$

$$\beta_h = 2/\{1 + 320\exp[-0.1(V + 75)]\}$$

$$\alpha_m = 0.2(V + 41)/[1 - \exp[-0.1(V + 41)]\}$$

$$\beta_m = 8\exp[-0.056(V + 66)]$$

$$V_{Na,K} = (RT/F) \cdot \log[([Na^+]_e + P_{Na,K}[K^+]_e)/([Na^+]_i + P_{Na,K}[K^+]_i)]$$

Sodium-calcium exchange current (i_{NaCa})

$$i_{NaCa} = k_{NaCa}\{[Ca^{2+}]_e[Na^+]_i^3 \exp[\gamma_{NaCa}V/(RT/F)] - [Ca^{2+}]_i[Na^+]_e^3 \exp[(\gamma_{NaCa} - 1)V/(RT/F)]\}/[1 + d_{NaCa}([Ca^{2+}]_e[Na^+]_i^3 + [Ca^{2+}]_i[Na^+]_e^3)]$$

Sodium-potassium pump current (i_{NaK})

$$i_{NaK} = [[Na^+]_i/([Na^+]_i + K_{m,Na})]\{1 - [(V - 40)/211]^2\}i_{NaK,max} \quad (17)$$

Background currents

$$i_{b,Ca} = g_{b,Ca}(V - V_{Ca}) \quad (18)$$

$$V_{Ca} = [RT/(2F)]\log([Ca^{2+}]_e/[Ca^{2+}]_i)$$

$$i_{b,K} = g_{b,K}[[K^+]_e/([K^+]_e + K_{m,b,K})] \cdot (V - V_K)/\{1 + \exp[2(V - V_K + 10)/(RT/F)]\}$$

$$i_{b,Na} = g_{b,Na}(V - V_{Na}) \quad (19)$$

Ion concentrations

$$d[Ca^{2+}]_i/dt = -i_{Ca,net}/(2V_iF) \quad (20)$$

$$d[Ca^{2+}]_{rel}/dt = (i_{tr} - i_{rel})/(2V_{rel}F)$$

$$d[Ca^{2+}]_{up}/dt = (i_{up} - i_{tr})/(2V_{up}F)$$

$$i_{Ca,net} = i_{b,Ca} + i_{Ca,L,Ca} + i_{Ca,T} - 2i_{NaCa} - i_{rel} + i_{up}$$

$$i_{rel} = a_{rel}[Ca^{2+}]_{rel}/[1 + (K_{m,Ca}/[Ca^{2+}]_i)^2]$$

$$i_{tr} = p\,a_{tr}([Ca^{2+}]_{up} - [Ca^{2+}]_{rel})$$

$$i_{up} = a_{up}[Ca^{2+}]_i([Ca^{2+}]_{up,max} - [Ca^{2+}]_{up})$$

$$\alpha_p = 0.000625(V + 64)/[\exp[0.25(V + 64)] - 1]$$

$$\beta_p = 0.005/[1 + \exp[-0.25(V + 64)]]$$

$$d[K^+]_i/dt = -i_{K,net}/(V_iF) \quad (21)$$

$$i_{K,net} = i_{Ca,L,K} + i_{f,K} + i_K + i_{b,K} + i_{Na} - 2i_{NaK}$$

$$d[Na^+]_i/dt = -i_{Na,net}/(V_iF) \quad (22)$$

$$i_{Na,net} = i_{b,Na} + i_{Ca,L,Na} + i_{f,Na} + i_{Na} + 3i_{NaCa} + 3i_{NaK}$$

Stable-start values of variables

$[Ca^{2+}]_i = 0.0000804$ mM	$f_L = 0.9973118$	$[Na^+]_i = 7.5$ mM
$[Ca^{2+}]_{rel} = 0.6093$ mM	$f_T = 0.1175934$	$p = 0.2844889$
$[Ca^{2+}]_{up} = 3.7916$ mM	$h = 0.1608417$	$x = 0.3294906$
$d_L = 0.0002914$	$[K^+]_i = 140$ mM	$y = 0.1135163$
$d_T = 0.0021997$	$m = 0.1025395$	$V = -60.03$ mV

This study was supported by the Netherlands Organization for Scientific Research (NWO) through the Foundation for Biophysics.

Received for publication 7 January 1991 and in final form 24 June 1991.

REFERENCES

Belardinelli, L., W. R. Giles, and A. West. 1988. Ionic mechanisms of adenosine actions in pacemaker cells from rabbit heart. *J. Physiol. (Lond.)*. 405:615–633.

Bleeker, W. K., A. J. C. Mackaay, M. Masson-Pévet, L. N. Bouman, and A. E. Becker. 1980. Functional and morphological organization of the rabbit sinus node. *Circ. Res.* 46:11–22.

Bonke, F. I. M., L. N. Bouman, and H. E. van Rijn. 1969. Change of cardiac rhythm in the rabbit after an atrial premature beat. *Circ. Res.* 24:533–544.

Bristow, D. G., and J. W. Clark. 1982. A mathematical model of primary pacemaking cell in SA node of the heart. *Am. J. Physiol.* 243:H207–H218.

Brown, H. F., and J. C. Denyer. 1990. Does a background inward current normally contribute to the pacemaker potential in rabbit isolated sino-atrial node cells? *J. Physiol. (Lond.)*. 423:62P.

Chapman, R. A., and D. Noble. 1989. Sodium-calcium exchange in the heart. *In* Sodium-calcium exchange. T. J. A. Allen, D. Noble, and H. Reuter, editors. Oxford University Press, New York. 102–125.

Denyer, J. C. 1989. Isolation and electrophysiological characteristics of rabbit sino-atrial node cells. Ph. D. Thesis. University of Oxford. 1–93.

Denyer, J. C., and H. F. Brown. 1990*a*. Rabbit sino-atrial node cells: isolation and electrophysiological properties. *J. Physiol. (Lond.)*. 428:405–424.

Denyer, J. C. and H. F. Brown. 1990*b*. Pacemaking in rabbit isolated sino-atrial node cells during Cs^+ block of the hyperpolarizing-activated current i_f. *J. Physiol. (Lond.)*. 429:401–409.

DiFrancesco, D. 1981. A new interpretation of the pace-maker current in calf Purkinje fibres. *J. Physiol. (Lond.)*. 314:359–376.

DiFrancesco, D., and D. Noble. 1985. A model of cardiac electrical activity incorporating ionic pumps and concentration changes. *Phil. Trans. R. Soc. Lond.* B307:353–398.

DiFrancesco, D., and D. Noble. 1989. Current i_f and its contribution to cardiac pacemaking. *In* Neuronal and Cellular Oscillators. J. W. Jacklet, editor. Marcel Dekker, Inc., New York. 31–57.

DiFrancesco, D., A. Ferroni, M. Mazzanti, and C. Tromba. 1986. Properties of the hyperpolarizing-activated current (i_f) in cells isolated from the rabbit sino-atrial node. *J. Physiol. (Lond.)*. 377:61–88.

Doerr, Th., R. Denger, and W. Trautwein. 1989. Calcium currents in single SA nodal cells of the rabbit heart studied with action potential clamp. *Pflügers Arch. Eur. J. Physiol.* 413:599–603.

Gadsby, D. C., J. Kimura, and A. Noma. 1985. Voltage dependence of Na/K pump current in isolated heart cells. *Nature (Lond.)*. 315:63–65.

Hagiwara, N., and H. Irisawa. 1988. Na-Ca exchange current in sinoatrial node cell of rabbit. *Circ. Suppl.* 78(2):123.

Hagiwara, N., H. Irisawa, and M. Kameyama. 1988. Contribution of two types of calcium currents to the pacemaker potentials of rabbit sino-atrial node cells. *J. Physiol. (Lond.)*. 395:233–253.

Hodgkin, A. L., amd A. F. Huxley. 1952. A quantitative description of membrane current and its application to conduction and excitation in nerve. *J. Physiol. (Lond.)*. 117:500–544.

Irisawa, H., and N. Hagiwara. 1988. Pacemaker mechanism of mammalian sinoatrial node cells. *In* Electrophysiology of the Sinoatrial and Atrioventricular Nodes. T. Mazgalev, L. S. Dreifus, and E. L. Michelson, editors. Alan R. Liss, Inc., New York. 33–52.

Irisawa, H., and A. Noma. 1982. Pacemaker mechanisms of rabbit sinoatrial node cells. *In* Cardiac rate and rhythm. L. N. Bouman, and H. J. Jongsma, editors. Martinus Nijhoff, London. 35–51.

Irisawa, H., T. Nakayama, and A. Noma. 1987. Membrane currents of single pacemaker cells from rabbit S-A and A-V nodes. *In* Electrophysiology of Single Cardiac Cells. D. Noble, and T. Powell, editors. Academic Press, New York. 167–186.

Irisawa, H., H. F. Brown, and W. R. Giles. 1991. Sino-atrial pacemaker mechanisms. *Physiol. Rev.* In press.

McAllister, R. E., D. Noble, and R. W. Tsien. 1975. Reconstruction of the electrical activity of cardiac Purkinje fibres. *J. Physiol. (Lond.)*. 251:1–59.

Nakayama T., Y. Kurachi, A. Noma, and H. Irisawa. 1984. Action potential and membrane currents of single pacemaker cells of the rabbit heart. *Pflügers Arch. Eur. J. Physiol.* 402:248–257.

Nathan, R. D. 1987. Role of i_f in pacemaker activity of the sinoatrial node. *Biophys. J.* 51:263a. (Abstr.)

Nilius, B. 1986. Possible functional significance of a novel type of cardiac Ca channel. *Biomed. Biochim. Acta.* 45:K37–K45.

Noble D., and S. J. Noble. 1984. A model of sino-atrial node electrical activity based on a modification of the DiFrancesco-Noble (1984) equations. *Proc. R. Soc. Lond. B Biol. Sci.* B222:295–304.

Noble, D., D. DiFrancesco, and J. C. Denyer. 1989. Ionic mechanisms in normal and abnormal cardiac pacemaker activity. *In* Neuronal and Cellular Oscillators. J. W. Jacklet, editor. Marcel Dekker, Inc., New York. 59–85.

Oei, H. I., A. C. G. van Ginneken, H. J. Jongsma, and L. N. Bouman. 1989. Mechanisms of impulse generation in isolated cells from the rabbit sinoatrial node. *J. Mol. Cell. Cardiol.* 21:1137–1149.

op 't Hof, T., B. de Jonge, A. J. C. Mackaay, W. K. Bleeker, M. Masson-Pévet, H. J. Jongsma, and L. N. Bouman. 1985. Functional and morphological organization of the guinea-pig sinoatrial node compared with the rabbit sinoatrial node. *J. Mol. Cell. Cardiol.* 17:549–564.

op 't Hof, T., A. C. G. van Ginneken, L. N. Bouman, and H. J. Jongsma. 1987. The intrinsic cycle length in small pieces isolated from the rabbit sinoatrial node. *J. Mol. Cell. Cardiol.* 19:923–934.

Reiner, V. S., and C. Antzelevitch. 1985. Phase resetting and annihilation in a mathematical model of sinus node. *Am. J. Physiol.* 249:H1143–H1153.

Shibasaki, T. 1987. Conductance and kinetics of delayed rectifier potassium channels in nodal cells of the rabbit heart. *J. Physiol. (Lond.).* 387:227–250.

van Ginneken, A. C. G., and W. R. Giles. 1991. Voltage clamp measurements of the hyperpolarization-activated inward current I_f in single cells from rabbit sino-atrial node. *J. Physiol. (Lond.).* 434:57–83.

Victorri, B., A. Vinet, F. A. Roberge, and J.-P. Drouhard. 1985. Numerical integration in the reconstruction of cardiac action potentials using Hodgkin-Huxley-type models. *Comp. Biomed. Res.* 18:10–23.

Yanagihara, K., A. Noma, and H. Irisawa. 1980. Reconstruction of sino-atrial node pacemaker potential based on the voltage clamp experiments. *Jpn. J. Physiol.* 30:841–857.